

Average Co magnetic moment of R-Co-B (R = Y, Pr and Nd) compounds

FUMIO MARUYAMA

177-11, Shimadachi, Matsumoto 390-0852, Japan

E-mail: fmaruya@shinshu-u.ac.jp

Published online: 08 July 2005

We estimate the average Co magnetic moment and account for the moment variation by a model in $Y_{n+1}Co_{3n+5}B_{2n}$ ($n = 0, 1, 2, 3$ and ∞), $Pr_{m+n}Co_{5m+3n}B_{2n}$ ($m = 2, n = 1$ and $m = 2, n = 3$), $Nd_{m+n}Co_{5m+3n}B_{2n}$ ($m = 3, n = 2$) and $Y_2Co_{14}B$ compounds. And we obtain the magnetic properties of hypothetical $Y_{m+n}Co_{5m+3n}B_{2n}$ ($n = 1, m = 2, 3, 4$ and 5) compounds.

© 2005 Springer Science + Business Media, Inc.

1. Introduction

In the case of R-Co-B (R = rare-earth) systems, it has been shown that a homologous series of compounds exists between the compositions RCO_5 and RCO_3B_2 . This series is represented by a general formula $R_{n+1}Co_{3n+5}B_{2n}$, which is formed by alternating stacking of one layer RCO_5 and n layers RCO_3B_2 along the c axis. The $R_{n+1}Co_{3n+5}B_{2n}$ compounds, where R is a rare earth or yttrium, crystallize in a hexagonal structure having the $P6/mmm$ space group and are known to exhibit a very interesting series of crystal structures with special atomic orderings depending on n [1–3]. The crystal structures of $R_{n+1}Co_{3n+5}B_{2n}$ ($n = 0, 1, 2, 3$ and ∞), $R_{m+n}Co_{5m+3n}B_{2n}$ ($m = 2, n = 1$ and $m = 2, n = 3$) and $R_2Co_{14}B$ are shown in Fig. 1. The $R_{n+1}Co_{3n+5}B_{2n}$ compounds with $n = 1$ (RCO_4B), $n = 2$ ($R_3Co_{11}B_4$), $n = 3$ ($R_2Co_7B_3$) and $n = \infty$ (RCO_3B_2) are derived from the RCO_5 structure by substituting B for Co at the $2c$ site [4]. For $R_{n+1}Co_{3n+5}B_{2n}$, there are three kinds of Co sites expressed by $Co(N)$ with $N = 1, 2$ and 3 , where $Co(N)$ means a Co atom which has N boron layers just above and/or just below. The RCO_4B compound has $Co(0)$ and $Co(1)$ sites. The $R_3Co_{11}B_4$ and $R_2Co_7B_3$ compounds have $Co(0)$, $Co(1)$ and $Co(2)$ sites. The RCO_3B_2 compound has only $Co(2)$ site and the average Co moment is very small [5].

New compounds $R_3Co_{13}B_2$ (R = Pr, Nd and Sm) [6–8], $R_5Co_{19}B_6$ (R = Pr and Nd) [6, 9] and $Nd_5Co_{21}B_4$ [10] have been synthesized successfully and belong to the $R_{m+n}Co_{5m+3n}B_{2n}$ family with $m = 2, n = 1, m = 2, n = 3$ and $m = 3, n = 2$, respectively. The crystal structure of $m = 3, n = 2$ is the same as that of $m = 2, n = 3$. While the $2d$ and $4h2$ sites are occupied by B and the $4h1$ site is occupied by Co in $m = 2, n = 3$, those by Co and that by B in $m = 3, n = 2$. Those crystallize in a hexagonal structure having the $P6/mmm$ space group and are crystallographically equivalent to $R_{n+1}Co_{3n+5}B_{2n}$, which is $R_{m+n}Co_{5m+3n}B_{2n}$ with $m = 1$. Those are formed by alternate stacking of m parts of RCO_5 with n parts of RCO_3B_2 along the c axis and are expected to show a

combination of high Curie temperature, large saturation magnetization and large magnetocrystalline anisotropy. The $R_3Co_{13}B_2$ and $R_5Co_{21}B_4$ compounds have $Co(0)$ and $Co(1)$ sites. The $R_5Co_{19}B_6$ compound has $Co(0)$, $Co(1)$ and $Co(2)$ sites.

The $R_2Co_{14}B$ compound crystallizes with a tetragonal structure having the $P4_2/mnm$ space group and has two rare-earth sites (4f and 4g), six Co sites (16k1, 16k2, 8j1, 8j2, 4e and 4c) and one boron site (4g). The $R_2Fe_{14}B$ compound is most attractive due to the industrial application for permanent magnets. There are four $R_2Co_{14}B$ units (68 atoms) per unit cell. All the R and B atoms, but only 4 of the 56 Co atoms, reside in the $z = 0$ and 0.5 planes. Between these the other Co atoms form puckered, yet fully connected, hexagonal nets. The tetragonal structure of $R_2Co_{14}B$ is closely related to the RCO_5 -type structure [11]. The B atom occupies the center of trigonal prism formed by the three nearest Co atoms above and the three below the plane containing B and R atoms. The prisms are strong structural units linking the Co planes above and below those containing R and B [12]. The prisms also coordinate all R and B atoms. Three R atoms are bonded to each B through the rectangular prism faces. Gaskell [13] has stressed that such trigonal prisms are fundamental to the structure of many transition metal—metalloid systems, both crystalline (e.g., FeB and Fe_3C) and amorphous.

In this work, we estimate the average Co magnetic moment and account for the moment variation by a model in $Y_{n+1}Co_{3n+5}B_{2n}$ ($n = 0, 1, 2, 3$ and ∞), $Pr_{m+n}Co_{5m+3n}B_{2n}$ ($m = 2, n = 1$ and $m = 2, n = 3$), $Nd_{m+n}Co_{5m+3n}B_{2n}$ ($m = 3, n = 2$) and $Y_2Co_{14}B$ compounds. And we obtain the magnetic properties of hypothetical $Y_{m+n}Co_{5m+3n}B_{2n}$ ($n = 1, m = 2, 3, 4$ and 5) compounds.

2. Results and discussion

2.1. Interatomic distance

We calculated the distances from each site to the neighboring atoms, d , and the number of the neighboring

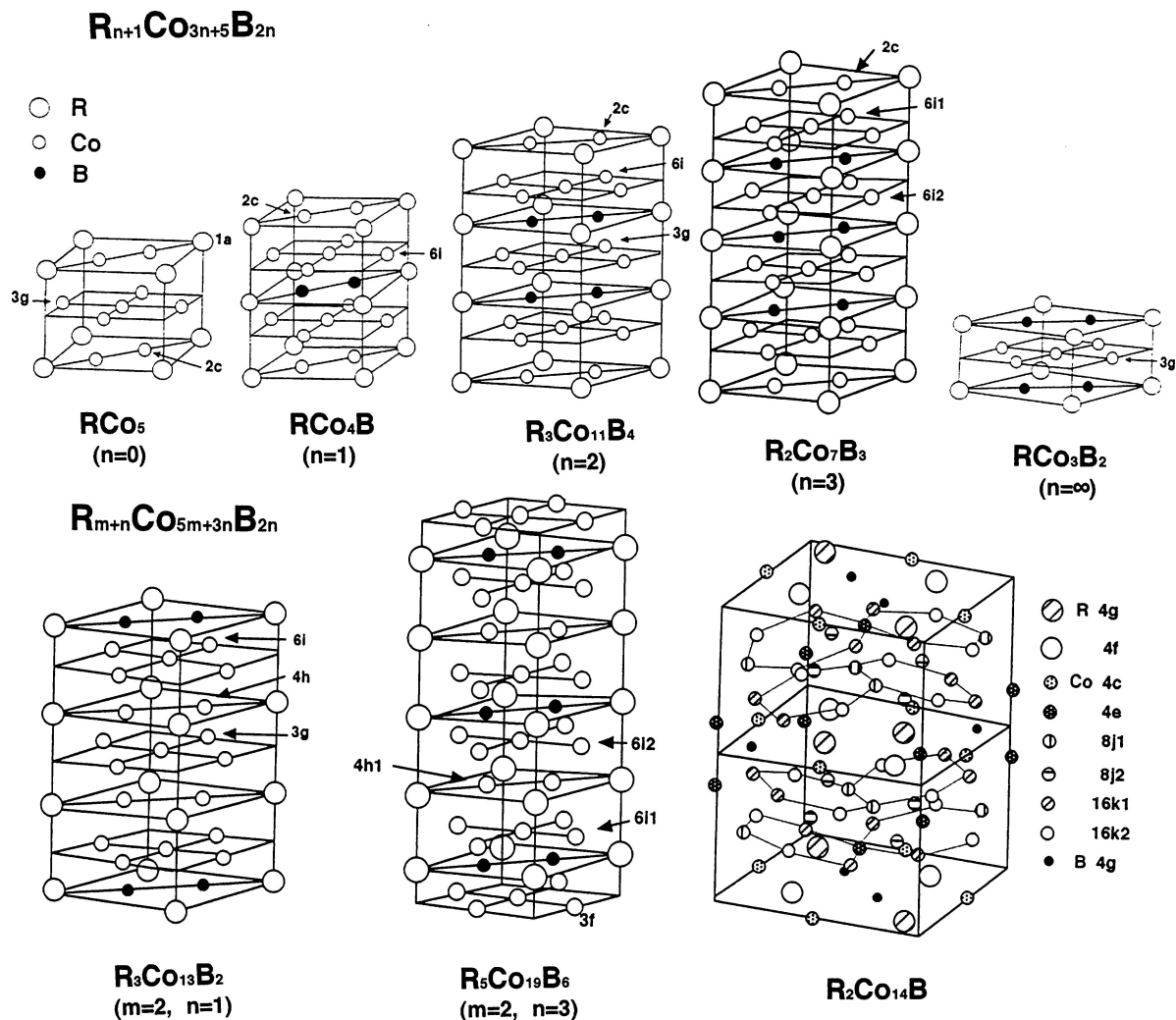


Figure 1 The crystal structure of $R_{n+1}Co_{3n+5}B_{2n}$ ($n = 0, 1, 2, 3$ and ∞), $R_{m+n}Co_{5m+3n}B_{2n}$ ($m = 2, n = 1$ and $m = 2, n = 3$) and $R_2Co_{14}B$.

atoms at each site, N , in $Y_{n+1}Co_{3n+5}B_{2n}$ ($n = 0, 1, 2, 3$ and ∞), $Pr_3Co_{13}B_2$, $Pr_5Co_{19}B_6$ and $Y_2Co_{14}B$. We used the results of Rietveld refinement for $Y_{n+1}Co_{3n+5}B_{2n}$ ($n = 0, 1, 2, 3$ and ∞) [14], $Pr_3Co_{13}B_2$ [6], $Pr_5Co_{19}B_6$ [8] and $Nd_2Fe_{14}B$ [11] and the values of the lattice constants for $Y_{n+1}Co_{3n+5}B_{2n}$ ($n = 0, 1, 2, 3$ and ∞), $Pr_3Co_{13}B_2$, $Pr_5Co_{19}B_6$ and $Y_2Co_{14}B$, which are from Refs. [5, 6, 8, 15], respectively. We also calculated the average distance from each Y (Pr), Co and B site to the neighboring Y (Pr), Co and B.

The dependence of the average distances from each Co site to the neighboring Co and B atoms, d_{Co-Co} and d_{Co-B} , and from each B site to the neighboring B atoms, d_{B-B} on the B concentration for $Y_{n+1}Co_{3n+5}B_{2n}$ ($n = 0, 1, 2, 3$ and ∞), $Pr_3Co_{13}B_2$, $Pr_5Co_{19}B_6$ and $Y_2Co_{14}B$ is shown in Fig. 2. The values of d_{Co-Co} and d_{Co-B} increase with increasing B concentration. The increase in d_{Co-Co} is larger than that in d_{Co-B} . The values of d_{B-B} decrease with increasing B concentration. The density, D , of $Y_{n+1}Co_{3n+5}B_{2n}$ ($n = 0, 1, 2, 3$ and ∞), $Y_3Co_{13}B_2$, $Y_5Co_{19}B_6$ and $Y_2Co_{14}B$ is also shown in Fig. 2. When we calculated the values of $Y_3Co_{13}B_2$ and $Y_5Co_{19}B_6$, we used the lattice constants of $Pr_3Co_{13}B_2$ and $Pr_5Co_{19}B_6$. The values of D decrease linearly with increasing B concentration and those of $Y_3Co_{13}B_2$, $Y_5Co_{19}B_6$ and $Y_2Co_{14}B$ are small in spite of small B concentration.

In $Y_{n+1}Co_{3n+5}B_{2n}$ ($n = 1, 2, 3$ and ∞), $Pr_3Co_{13}B_2$, $Pr_5Co_{19}B_6$ and $Y_2Co_{14}B$, trigonal prism containing B atom exists and that in the YCo_4B structure is shown in Fig. 3. The B atom occupies the center of trigonal prism formed by the three nearest Co atoms above and the three below the plane containing B and R. The distances between the B(2d) atom and its nearest neighbors are $B-Co(6i) = 2.05 \text{ \AA}$, $B-Co(6i) = 2.08 \text{ \AA}$, $B-Y(1b) = 2.92 \text{ \AA}$ and $B-Y(1b) = 2.88 \text{ \AA}$. The vertical edge length is $Co(6i)-Co(6i) = 2.93 \text{ \AA}$. Distance in the triangular face is $Co(6i)-Co(6i) = 2.51 \text{ \AA}$. The values above are almost the same values in $Y_{n+1}Co_{3n+5}B_{2n}$ ($n = 2, 3$ and ∞), $Pr_3Co_{13}B_2$ and $Pr_5Co_{19}B_6$. In $Y_2Co_{14}B$, the distances between the B(4g) atom and its nearest neighbors are $B-Co(16k1) = 2.02 \text{ \AA}$, $B-Co(4e) = 2.08 \text{ \AA}$, $B-Y(4g) = 2.79 \text{ \AA}$ and $B-Y(4f) = 3.28 \text{ \AA}$. The vertical edge lengths are $Co(4e)-Co(4e) = 2.64 \text{ \AA}$ and $Co(16k1)-Co(16k1) = 3.00 \text{ \AA}$. Distances in the triangular face are $Co(16k1)-Co(4e) = 2.45 \text{ \AA}$ and $Co(16k1)-Co(16k1) = 2.53 \text{ \AA}$.

2.2. The average Co magnetic moment

The dependence of the average magnetic moment per Co atom, μ_{Co} , and Curie temperature, T_c , on the B concentration for $Y_{n+1}Co_{3n+5}B_{2n}$ ($n = 0, 1, 2,$

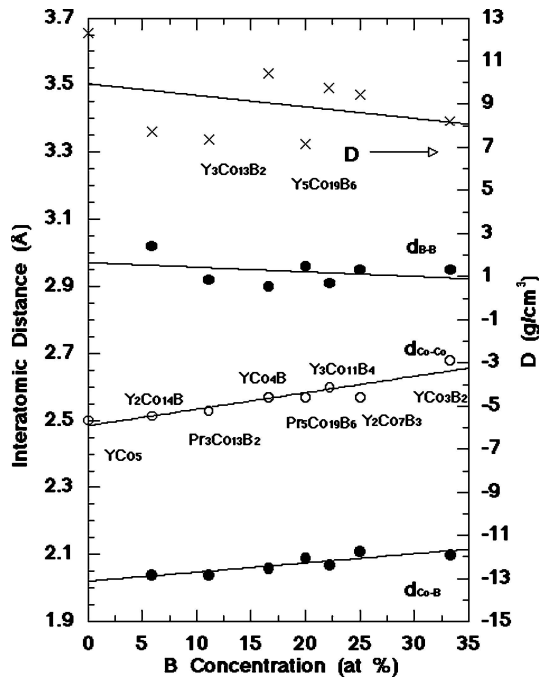


Figure 2 The dependence of the average distances from each Co site to the neighboring Co and B atoms, $d_{\text{Co-Co}}$ and $d_{\text{Co-B}}$, and from each B site to the neighboring B atoms, $d_{\text{B-B}}$ on the B concentration for $Y_{n+1}\text{Co}_{3n+5}\text{B}_{2n}$ ($n = 0, 1, 2, 3$ and ∞), $\text{Pr}_3\text{Co}_{13}\text{B}_2$, $\text{Pr}_5\text{Co}_{19}\text{B}_6$ and $\text{Y}_2\text{Co}_{14}\text{B}$. The density, D , of $Y_{n+1}\text{Co}_{3n+5}\text{B}_{2n}$ ($n = 0, 1, 2, 3$ and ∞), $\text{Y}_3\text{Co}_{13}\text{B}_2$, $\text{Y}_5\text{Co}_{19}\text{B}_6$ and $\text{Y}_2\text{Co}_{14}\text{B}$ is also shown.

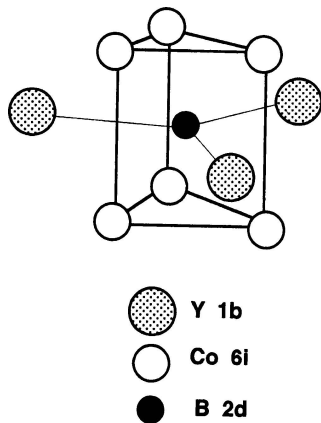


Figure 3 Trigonal prism containing a boron atom in the YCo_4B structure.

3 and ∞), $\text{Pr}_3\text{Co}_{13}\text{B}_2$, $\text{Pr}_5\text{Co}_{19}\text{B}_6$ and $\text{Y}_2\text{Co}_{14}\text{B}$ is shown in Fig. 4. The values of μ_{Co} and T_c for YCo_5 , YCo_4B , $\text{Y}_3\text{Co}_{11}\text{B}_4$, $\text{Y}_2\text{Co}_7\text{B}_3$, $\text{Pr}_3\text{Co}_{13}\text{B}_2$, $\text{Pr}_5\text{Co}_{19}\text{B}_6$ and $\text{Y}_2\text{Co}_{14}\text{B}$ are from Refs. [16], [5, 17], [5, 18], [5, 19], [6], [8] and [15], respectively. The values of μ_{Co} for Pr compounds [6, 8] are obtained by assuming that the average Pr^{3+} moment to be $2.4 \mu_B$. The values of μ_{Co} decrease almost linearly with increasing B concentration, that is, the values of $d_{\text{Co-Co}}$. The values of T_c also decrease with increasing B concentration. Those for YCo_5 and $\text{Y}_2\text{Co}_{14}\text{B}$ are large. For the other compounds, those are small and the value of $\text{Pr}_3\text{Co}_{13}\text{B}_2$ is small comparing with those of other compounds. The dependence of the average magnetic moment per Co atom, μ_{Co} , and Curie temperature, T_c , on the average number of the nearest neighbor Co atoms at each site, $N(\text{Co})$, for $Y_{n+1}\text{Co}_{3n+5}\text{B}_{2n}$ ($n = 0, 1, 2, 3$ and ∞), $\text{Pr}_3\text{Co}_{13}\text{B}_2$, $\text{Pr}_5\text{Co}_{19}\text{B}_6$ and $\text{Y}_2\text{Co}_{14}\text{B}$ is shown in Fig. 5.

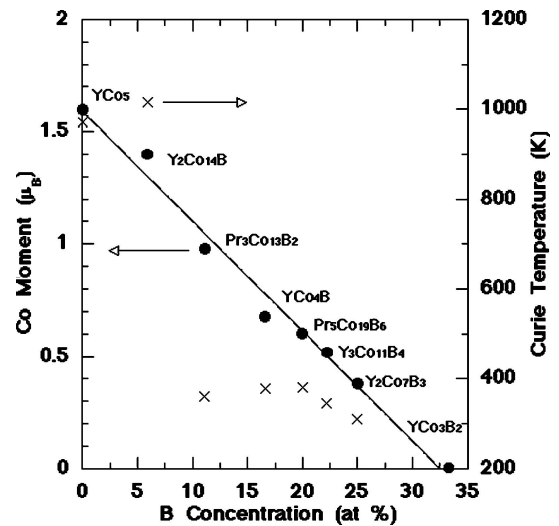


Figure 4 The dependence of the average magnetic moment per Co atom and Curie temperature on the B concentration for $Y_{n+1}\text{Co}_{3n+5}\text{B}_{2n}$ ($n = 0, 1, 2, 3$ and ∞), $\text{Pr}_3\text{Co}_{13}\text{B}_2$, $\text{Pr}_5\text{Co}_{19}\text{B}_6$ and $\text{Y}_2\text{Co}_{14}\text{B}$.

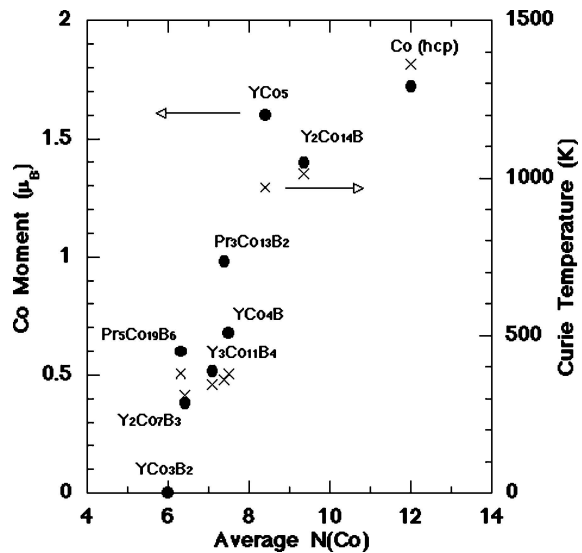


Figure 5 The dependence of μ_{Co} and T_c on the average number of the nearest neighbor Co atoms at each site, $N(\text{Co})$, for $Y_{n+1}\text{Co}_{3n+5}\text{B}_{2n}$ ($n = 0, 1, 2, 3$ and ∞), $\text{Pr}_3\text{Co}_{13}\text{B}_2$, $\text{Pr}_5\text{Co}_{19}\text{B}_6$ and $\text{Y}_2\text{Co}_{14}\text{B}$.

The values of μ_{Co} and T_c increase with increasing the values of $N(\text{Co})$. Hence, the increased $N(\text{Co})$ and the decreased $d_{\text{Co-Co}}$ enhance the values of μ_{Co} and T_c .

The concentration of the numbers of Co(0), Co(1) and Co(2) sites versus the average Co moment for $Y_{n+1}\text{Co}_{3n+5}\text{B}_{2n}$ ($n = 0, 1, 2, 3$ and ∞), $\text{Pr}_{m+n}\text{Co}_{5m+3n}\text{B}_{2n}$ ($m = 2, n = 1$ and $m = 2, n = 3$) and $\text{Nd}_{m+n}\text{Co}_{5m+3n}\text{B}_{2n}$ ($m = 3, n = 2$) are shown in Fig. 6. The average Co moment increases with increasing the Co(0) concentration and decreases with increasing the Co(2) one.

2.3. A model of the moment variation in $Y_{n+1}\text{Co}_{3n+5}\text{B}_{2n}$ ($n = 0, 1, 2, 3$ and ∞), $\text{Pr}_{m+n}\text{Co}_{5m+3n}\text{B}_{2n}$ ($m = 2, n = 1$ and $m = 2, n = 3$), $\text{Nd}_{m+n}\text{Co}_{5m+3n}\text{B}_{2n}$ ($m = 3, n = 2$) and $\text{Y}_2\text{Co}_{14}\text{B}$ compounds. We consider a model focus on boron coordination in explaining magnetic moments in those compounds. The

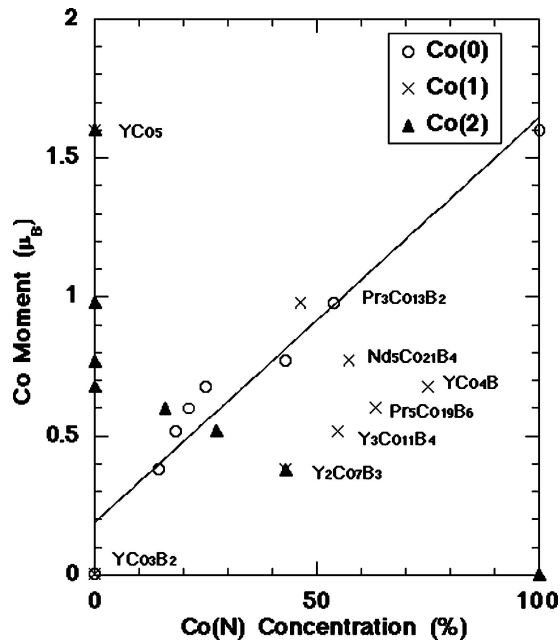


Figure 6 The concentration of the numbers of Co(0), Co(1) and Co(2) sites versus the average Co moment for $Y_{n+1}Co_{3n+5}B_{2n}$ ($n = 0, 1, 2, 3$ and ∞), $Pr_3Co_{13}B_2$, $Pr_5Co_{19}B_6$ and $Nd_5Co_{21}B_4$.

extent of p-d bonding is assumed to be proportional to the number of T (transition-metal) atoms surrounding an M (metalloid) atom, Z . If the T atom is strongly ferromagnetic with a magnetization at 0 K of n_B , the magnitude of the average magnetic moment μ per T atom in the alloy is shown as below [20]:

$$\mu = n_B - Z(n_B/5)(N_M/N_T), \quad (1)$$

where N_M/N_T is the ratio of the number of M atoms to T atoms. Equation 1 assumes that each of the Z nearest-neighbor T atoms forms a bond with the central M atom and therefore loses, on average, one fifth of its moment because one of its five 3d electron orbitals is tied up in a nonmagnetic, covalent bond.

We show the average Co magnetic moment, μ_{Co} , as a function of concentration N_B/N_{Co} for $Y_{n+1}Co_{3n+5}B_{2n}$ ($n = 0, 1, 2, 3$ and ∞), $Pr_{m+n}Co_{5m+3n}B_{2n}$ ($m = 2, n = 1$ and $m = 2, n = 3$), $Nd_{m+n}Co_{5m+3n}B_{2n}$ ($m = 3, n = 2$) and $Y_2Co_{14}B$ compounds in Fig. 7. The values of μ_{Co} for YCo_5 , YCo_4B , $Y_3Co_{11}B_4$, $Y_2Co_7B_3$, YCo_3B_2 , $Pr_3Co_{13}B_2$, $Pr_5Co_{19}B_6$, $Nd_5Co_{21}B_4$ and $Y_2Co_{14}B$ are from Refs. [16], [5], [5], [5], [5], [6], [9], [10] and [15], respectively. The values of μ_{Co} for Pr [6, 8] and Nd [10] compounds are obtained by assuming that the average Pr^{3+} and Nd^{3+} moment to be 2.4 and 3.0 μ_B , respectively. The value of n_B was taken as 1.72 μ_B for hcp Co. The value of μ_{Co} does not decrease linearly with increasing that of N_B/N_{Co} . Line a is a model in Equation 1, where Z is six, and departs from the values of μ_{Co} . So, we must change the value of Z in Equation 1 to fit the values of μ_{Co} . Line B is calculated using a least-squares program for $0 \leq N_B/N_{Co} \leq 0.66$ and the value of Z is 9.1, but the line does not fit the values of μ_{Co} . In all regions, a line can not be drawn and there are two slopes. Next, we obtained line c using a least-squares program for $0 \leq N_B/N_{Co} \leq 0.25$. The line fits

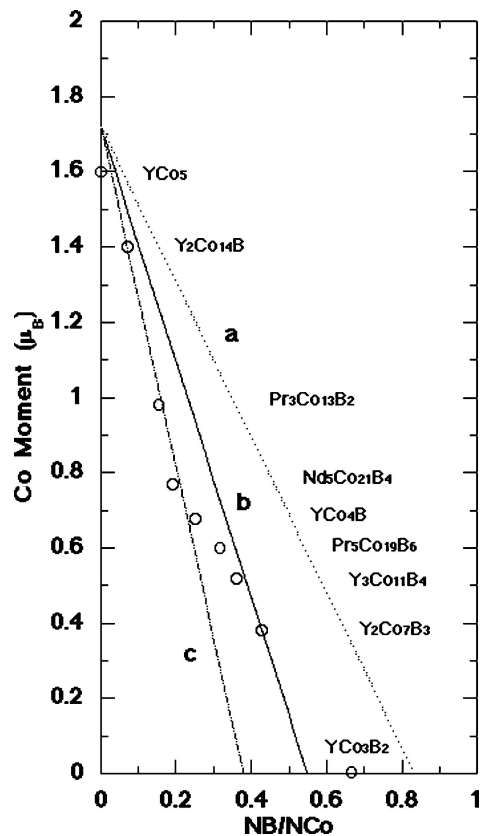


Figure 7 Average Co magnetic moment as a function of concentration N_B/N_{Co} for $Y_{n+1}Co_{3n+5}B_{2n}$ ($n = 0, 1, 2, 3$ and ∞), $Pr_3Co_{13}B_2$, $Pr_5Co_{19}B_6$, $Nd_5Co_{21}B_4$ and $Y_2Co_{14}B$ compounds. Line a is a model in Equation 1. Lines B and c are calculated using a least-squares program for $0 \leq N_B/N_{Co} \leq 0.66$ and for $0 \leq N_B/N_{Co} \leq 0.25$, respectively.

the values of μ_{Co} well and the value of Z is 13.2. Consequently, the value of Z is varied continuously from 13.2 for $0 \leq N_B/N_{Co} \leq 0.25$ to 9.1 for $0 \leq N_B/N_{Co} \leq 0.66$. The value of Z is near 13.2 and a boron atom bonds with 13.2 Co atoms for $Y_2Co_{14}B$, $Pr_3Co_{13}B_2$, $Nd_5Co_{21}B_4$ and YCo_4B . The value of Z is near 9.1 and a boron atom bonds with 9.1 Co atoms for $Pr_5Co_{19}B_6$, $Y_3Co_{11}B_4$ and $Y_2Co_7B_3$. Consequently, the extent of p-d bonding becomes large with decreasing the value of N_B/N_{Co} and gives rise to a sharper moment reduction. The value of Z is large comparing with that obtained from structural analysis. While we assume that T atom loses one fifth of its moment, T atom is considered to lose more its moment.

2.4. The magnetic properties of hypothetical $Y_{m+n}Co_{5m+3n}B_{2n}$ ($n = 1, m = 2, 3, 4$ and 5) compounds

The $Y_2Co_{14}B$ compound is most similar to $Pr_3Co_{13}B_2$ among $Y_{n+1}Co_{3n+5}B_{2n}$ ($n = 0, 1, 2, 3$ and ∞) and $Pr_{m+n}Co_{5m+3n}B_{2n}$ ($m = 2, n = 1$ and $m = 2, n = 3$) compounds, considering B concentration and Co moment. Here, increasing m from 2 to 5 with $n = 1$, the B concentration decreases and that of $m = 5$ is almost equal to that of $Y_2Co_{14}B$ and the comparison of those compounds with $Y_2Co_{14}B$ is very interesting. Hence, we estimate the Co moment for hypothetical $Y_{m+n}Co_{5m+3n}B_{2n}$ ($n = 1, m = 2, 3, 4$ and 5) compounds, which are $Y_3Co_{13}B_2$, Y_2Co_9B , $Y_5Co_{23}B_2$ and

$Y_3Co_{14}B$, respectively. Those are formed by alternate stacking of m parts of RCO_5 with one part of RCO_3B_2 along the c axis. The B atoms reside only in the $z = 0$ and 1 planes. Those compounds have Co(0) and Co(1) sites. The values of μ_{Co} at the 2c site, which is Co(0) site, and 6i site, which is Co(1) site, for YCo_4B obtained by neutron powder diffraction are 1.5 and 0.5 μ_B , respectively [9], and we used the values. So the calculated values of μ_{Co} are 1.0, 1.2, 1.2 and 1.3 μ_B for $Y_3Co_{13}B_2$, Y_2Co_9B , $Y_5Co_{23}B_2$ and $Y_3Co_{14}B$, respectively. The value of μ_{Co} decreases almost linearly with increasing B concentration. The B concentration for $Y_2Co_{14}B$ (5.88%) is almost equal to that for $Y_3Co_{14}B$ (5.55%). The values of μ_{Co} for $Y_2Co_{14}B$ and $Y_3Co_{14}B$ are 1.4 and 1.3 μ_B , respectively.

Next, we estimate the magnetic anisotropy for hypothetical $Y_{m+n}Co_{5m+3n}B_{2n}$ ($n = 1, m = 2, 3, 4$ and 5) compounds. The NMR study of RCO_5 by Streever [21] indicated that the spin-orbit magnetic moment of Co atom at the 2c site contributes significantly to the anisotropy of RCO_5 . The uniaxial magnetization direction of RCO_5 stems from Co atoms at the 2c site and Co atoms at the 3g site exert a relatively small reverse contribution [21]. Moreover to study the Co contribution to the magnetic anisotropy, we calculate the total anisotropy energy, E_A , using the local anisotropy energy per Co atom, E_s , of the hypothetical $Y_{m+n}Co_{5m+3n}B_{2n}$ ($n = 1, m = 2, 3, 4$ and 5) compounds, which are $Y_3Co_{13}B_2$, Y_2Co_9B , $Y_5Co_{23}B_2$ and $Y_3Co_{14}B$, respectively. We used the values of E_s in YCo_5 [21] and $Y_3Co_{11}B_4$ [22]. In YCo_5 , the values of E_s at the 2c and 3g sites, being Co(0) site, are 24 and -7 $cm^{-1}/atom$, respectively. In YCo_5 , the net calculated anisotropy energy is 27 $cm^{-1}/unit$ cell or about 6.4×10^7 erg/cm^3 . This is close to the measured low temperature anisotropy energy K_1 of 7.5×10^7 erg/cm^3 for YCo_5 [23]. It appears then that the single-ion anisotropy could explain most of the anisotropy of the compound [24]. In $Y_3Co_{11}B_4$, the values of E_s at the 6i1 site, being Co(1) site, and the 6i2 site, being Co(2) site, are -8.1 and 0.69 $cm^{-1}/atom$, respectively. Then

$$\begin{aligned} E_A(Y_3Co_{13}B_2) &= 3E_s(3g) + 4E_s(4h) + 6E_s(6i) \\ &= 26.4 \text{ cm}^{-1}/\text{unit cell}, \end{aligned} \quad (2)$$

where $E_s(4h) = E_s(2c)$ and $E_s(6i) = E_s(6i1)$. The calculated values of E_A for Y_2Co_9B , $Y_5Co_{23}B_2$ and $Y_3Co_{14}B$ are 53.4, 80.4 and 107.4 $cm^{-1}/unit$ cell, respectively.

Similarly, the calculated values of E_A for hypothetical $Y_{m+n}Co_{5m+3n}B_{2n}$ ($m = 2, n = 3$ and $m = 3, n = 2$) compounds, which are $Y_5Co_{19}B_6$ and $Y_5Co_{21}B_4$, are -1.2 and 46.8 $cm^{-1}/unit$ cell, respectively. The dependence of the value of E_A and the average E_s on the B concentration for hypothetical $Y_{m+n}Co_{5m+3n}B_{2n}$ ($n = 1, m = 2, 3, 4$ and 5), hypothetical $Y_{m+n}Co_{5m+3n}B_{2n}$ ($m = 2, n = 3$ and $m = 3, n = 2$) and $Y_2Co_{14}B$ [25] compounds is shown in Fig. 8. The average E_s decreases with increasing B concentration except for that of $Y_2Co_{14}B$.

The easy magnetization direction in $Pr_3Co_{13}B_2$ from 5 K to room temperature is parallel to the c axis [6]

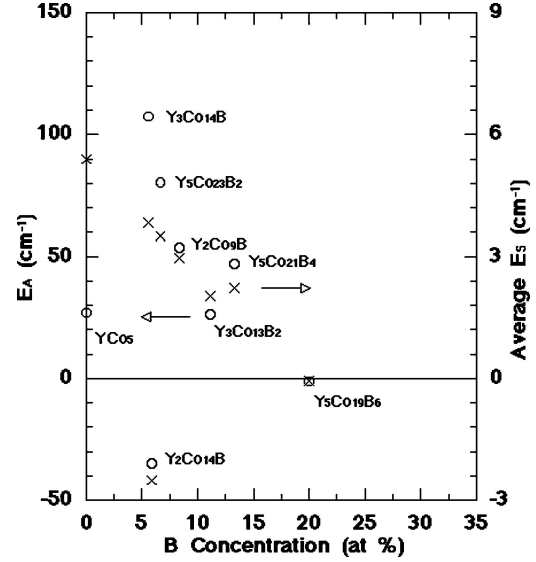


Figure 8 The dependence of the value of E_A and the average E_s on the B concentration for hypothetical $Y_{m+n}Co_{5m+3n}B_{2n}$ ($n = 1, m = 2, 3, 4$ and 5), hypothetical $Y_{m+n}Co_{5m+3n}B_{2n}$ ($m = 2, n = 3$ and $m = 3, n = 2$) and $Y_2Co_{14}B$ compounds.

and is explained as below. In $R_{m+n}Co_{5m+3n}B_{2n}$, the sign of A_2^0 is negative [3], which means that the R ion having a negative second-order Stevens coefficient α_J (Pr^{3+} , Nd^{3+}) shows planar anisotropy. The magnetic anisotropy results from a competition between the planar anisotropy of the Pr ions and the uniaxial one of the Co sublattice. The axial anisotropy of Co atoms is large, hence the $Pr_3Co_{13}B_2$ compound has axial anisotropy. In $R_{m+n}Co_{5m+3n}B_{2n}$, the R ion having a positive α_J (Sm^{3+}) shows axial anisotropy. The magnetic anisotropy of R in the plane containing B atoms is strengthened by B atoms as explained below. The R atom is surrounded by B atoms in the c plane. Assuming that B atom has a negative charge, the 4f electrons in R atom are distributed avoiding B atoms. From the schematic distributions of the wave functions of the 4f electrons in Sm , the axial anisotropy strengthens. Consequently, the $Sm_{m+n}Co_{5m+3n}B_{2n}$ compounds with large B concentration are expected to have large axial anisotropy.

3. Conclusions

In this work, we estimate the average Co magnetic moment and account for the moment variation by a model in $Y_{n+1}Co_{3n+5}B_{2n}$ ($n = 0, 1, 2, 3$ and ∞), $Pr_{m+n}Co_{5m+3n}B_{2n}$ ($m = 2, n = 1$ and $m = 2, n = 3$), $Nd_{m+n}Co_{5m+3n}B_{2n}$ ($m = 3, n = 2$) and $Y_2Co_{14}B$ compounds. And we obtain the magnetic properties of hypothetical $Y_{m+n}Co_{5m+3n}B_{2n}$ ($n = 1, m = 2, 3, 4$ and 5) compounds.

(1) The values of d_{Co-Co} and d_{Co-B} , the average distances from each Co site to the neighboring Co and B atoms, increase with increasing B concentration.

(2) The values of μ_{Co} decrease almost linearly with increasing B concentration, that is, the values of d_{Co-Co} . The values of Tc also decrease with increasing B concentration. The values of μ_{Co} and Tc increase with increasing the values of $N(Co)$, the average

number of the nearest neighbor Co atoms at each site.

(3) The extent of p-d bonding becomes large with decreasing the value of N_B/N_{Co} , the ratio of the number of B atoms to Co atoms and gives rise to a sharper moment reduction.

(4) The B concentration for $Y_2Co_{14}B$ is almost equal to that for hypothetical $Y_3Co_{14}B$. The value of μ_{Co} is $1.4 \mu_B$ for $Y_2Co_{14}B$ and the calculated value of μ_{Co} is $1.3 \mu_B$ for $Y_3Co_{14}B$.

(5) The average Es decreases with increasing B concentration for hypothetical $Y_{m+n}Co_{5m+3n}B_{2n}$ ($n = 1, m = 2, 3, 4$ and 5) and hypothetical $Y_{m+n}Co_{5m+3n}B_{2n}$ ($m = 2, n = 3$ and $m = 3, n = 2$) compounds.

References

1. H. OSTERREICHER, F. T. PARKAR and M. MISROCH, *Appl. Phys.* **12** (1977) 287.
2. Y. B. KUZMA, N. S. BILONIZHKO, S. I. MYKHALENKO, G. F. STEPANOVA and N. F. CHABAN, *J. Less-Common Met.* **67** (1979) 51.
3. H. H. SMIT, R. C. THIEL and K. H. J. BUSCHOW, *J. Phys. F* **18** (1988) 295.
4. Y. B. KUZMA and N. S. BILONIZHKO, *Sov. Phys. Crystallogr.* **18** (1974) 447.
5. H. IDO, *Kotai Butsuri* **30** (1995) 875 [in Japanese].
6. Y. CHEN, J. K. LIANG, X. L. CHEN, Q. L. LIU, B. G. SHEN and Y. P. SHEN, *J. Phys.: Condens. Matter* **11** (1999) 8251.
7. Y. CHEN, Q. L. LIU, J. K. LIANG, X. L. CHEN, B. G. SHEN and F. HUANGI, *Appl. Phys. Lett.* **74** (1999) 856.
8. Y. CHEN, X. LI, X. L. CHEN, J. K. LIANG, G. H. RAO and Q. L. LIU, *J. Alloys Compd.* **305** (2000) 216.
9. Y. CHEN, X. L. CHEN, J. K. LIANG B. G. SHEN and Q. L. LIU, *Phys. Rev.* **B61** (2000) 3502.
10. W. G. CHU, G. H. RAO, H. F. YANG, G. Y. LIU and J. K. LIANG, *J. Appl. Phys.* **90** (2001) 1931.
11. D. GIVORD, H. S. LI and J. M. MOREAU, *Solid State Commun.* **50** (1984) 497.
12. J. F. HERBST, J. J. CROAT and F. E. PINKERTON, *Phys. Rev.* **B29** (1984) 4176.
13. P. H. GASKELL, *Nature* **289** (1981) 47.
14. A. SZAJEK, *J. Magn. Magn. Mater.* **185** (1998) 322.
15. K. H. J. BUSCHOW, D. B. DE MOOIJ, S. SINNEMA, R. J. RADWANSKI and J. J. M. FRANSE, *ibid.* **51** (1985) 211.
16. K. H. J. BUSCHOW, *Rep. Prog. Phys.* **40** (1977) 1179.
17. H. S. LI and J. M. D. COEY, "Handbook of Magnetic Materials," edited by K. H. J. Buschow (North-Holland, Amsterdam, 1991) Vol. 6, p. 1.
18. A. KOWALCZYK, *J. Magn. Magn. Mater.* **136** (1994) 70.
19. *Idem.*, *ibid.* **175** (1997) 279.
20. B. W. CORB, C. O' HANDLEY and N. J. GRANT, *Phys. Rev.* **B27** (1983) 636.
21. R. L. STREEVER, *ibid.* **B19** (1979) 2704.
22. A. KOWALCZYK, *Phys. Stat. Sol. (b)* **181** (1994) K73.
23. G. HOFFER and K. STRNAT, *J. Appl. Phys.* **38** (1967) 1377.
24. R. L. STREEVER, *Phys. Lett.* **A65** (1978) 360.
25. N. P. THUY, T. D. HIEN, N. M. HONG and J. J. M. FRANSE, *J. de Phys.* **49** (1988) C8-579.

Received 7 December 2004
and accepted 22 February 2005